Single particle spectrum of a nucleon in the harmonic oscillator mean field with spin-orbit coupling - a semiclassical view

R. Gupta[a] and S. Sunder Malik[b]

[a]Department of Physics, Swami Swatantranand Memorial College, Dinanagar 143531 India.
e-mail: rajivguptamirage@gmail.com
[b]Department of Physics, Guru Nanak Dev University, Amritsar 143005 India.

We have presented the single, particle spectrum for a particle in a mean-field of an isotropic harmonic oscillator with $\vec{l}\cdot\vec{s}$ coupling based on our semiclassical approach. It has been seen that this spectrum, without $\vec{l}\cdot\vec{s}$ coupling, exactly matches with the quantum mechanical one (without nuclear constraints). In this case, periodicity conditions give only pendulating orbits coinciding with $l = 0$ axis, which fully supports the observations reported by Bohr and Mottelson [28]. The orbits with $l \geq 0$ are generated by reflecting the particle from the nuclear surface, R_0, instead of infinity, which is the usual nuclear constraint. The mean-field strength is fixed by virial theorem. The resulting spectrum compares reasonably with the quantum spectrum for a particle enclosed in a perfectly reflecting walls. The variation of particle number with energy helps us to identify the significant quantum numbers 'n' and 'l' in this semiclassical method. Finally, the $\vec{l}\cdot\vec{s}$ coupling splits each level and the splitting width of these levels compares well with that of nuclear splitting. Thus the complete nuclear shell model (with magic numbers) is reproduced without any fitting parameter.

Keywords: Semiclassical methods; periodic orbit theory; trace formula; spherical cavity.

PACS: 03.65.Sq; 03.65.Bz; 71.20.Ad; 05.45.+b   *DOI:* https://doi.org/10.31349/RevMexFis.66.82

1. Introduction

During the past decade, a variety of nuclear phenomena like magnetic rotation [1], chiral twin bands [2], shape coexistence [3,4], superheavy elements [5] and superdeformation [6] have been observed, which originate from single-particle and collective motion as well as their interplay. Traditionally, Strutinsky's shell correction method [7] has been one of the central approaches for calculation of potential energy surfaces [8,9,2], which is a key to understand these phenomena. This method, also known as the macroscopic plus microscopic approach, obtains the fluctuating part of the level density (the shell correction term) arising from the quantal shell correction energy. Parallel to Strutinsk's method, semiclassical methods have been developed [10-12], which can explain successfully the features of both ordered and chaotic quantum systems. Recently, the mixing of deuteron states ($^3S_1$ and $^3D_1$) with tensor interaction has been semiclassically analyzed [13].

One such semiclassical technique, known as periodic orbit theory (POT), was initiated nearly four decades ago by Gutzwiller [10], it has emerged as one of the most powerful methods of understanding the quantum spectra. Semiclassical trace formula, the as developed by Gutzwiller [14] for the fluctuating part of level density of a quantum system is given by

$$\delta_g(E) = \frac{1}{\pi\hbar} \sum_{PO} \frac{T_{PPO}}{\sqrt{det|\tilde{M}_{PO} - I|}}$$
$$\times \cos\left(\frac{S_{PO}}{\hbar} - \sigma_{PO}\frac{\pi}{2}\right) \qquad (1)$$

The left-hand side of Eq. (1) is a quantum mechanical quantity, whereas the right-hand side contains only the classical quantities. Here, T_{PPO} represents the time period of the primitive periodic orbit, and $\tilde{M}_{PO}$ is the monodromy stability matrix. The oscillations are controlled by action S_{PO} of each periodic orbit and σ_{PO} is a Maslov index. This trace formula is, however, applicable if all the periodic orbits are isolated.

Subsequently, several extensions of Gutzwiller's semiclassical trace formula were made to include regular and mixed dynamics for explaining quantum shell effects in many physical systems [15-18]. One such generalization was reported by Strutinsky *et al.* [19] to systems with continuous symmetries by explicitly taking into account the degeneracy of the classical orbits. This method was successfully applied to phenomenological potentials used in nuclear physics [19], yielding a semiclassical interpretation of ground-state deformation as a function of particle number. One of us [20] has also obtained an eigenvalue spectrum for a particle enclosed in an infinitely high spheroidal cavity by using the formalism of Strutinsky *et al.* On comparing this semiclassical eigenvalue spectrum with corresponding quantum mechanical values [21], we have established the importance and significant contribution of planar (both in the axis of symmetry plane and the equatorial plane) and 3-dimensional orbits for the normal deformed and the superdeformed regions. Further, this semiclassical method has been extended [22] to explain elegantly the mass asymmetry in nuclear fission [23].

Amann and Brack [24] have developed trace formula for a nuclear system in a 3-dimensional harmonic oscillator mean-field with a spin-orbit interaction of Thomas type. In the strong coupling limit, singularities occur in phase space where the spin-orbit interaction locally becomes zero. These

singularities impose severe restrictions on the applicability of the trace formula. However, they have pointed out that the leading orbits with shortest periods are free from singularities and lead to excellent results for the coarse-grained level density, as long as bifurcations of these orbits are avoided.

It is worthwhile to mention here that Littlejohn and Flynn [25] developed a semiclassical theory of systems with multi-component wavefunctions and applied [26] it to the WKB quantization of integrable spherical systems with the standard spin-orbit interactions. Frisk and Guhr [27] have studied the deformed systems with spin-orbit interaction by approximating the Schrodinger equation semiclassically. Here, the information about the periodic orbits is extracted from the Fourier transform of the quantum mechanical spectra.

The present work aims to obtain the complete spectrum for a particle moving in an isotropic three-dimensional harmonic oscillator mean-field with spin-orbit interaction. This work is based on the formalism developed by Strutinsky *et al.* [19]. The semiclassical interpretation for a nucleon in an isotropic oscillator mean-field was first given by Bohr and Mottelson [28]. They pointed out that only the pendulating orbits (also known as diametric orbits) are possible in this potential. These orbits are traced by a particle by executing two radial oscillations for each angular motion (*i.e.* $(\omega_r/\omega_\theta = 1/2)$. Such a trajectory coincides with $l = 0$ axis. We will show that our periodicity condition confirms their observation, and the calculated eigenvalue spectrum is exactly in agreement with a quantum mechanical one.

Further, the effect of spin-orbit coupling in the mean-field arises only if there is a contribution of orbits with $l \geq 0$. Such trajectories are obtained in our trace formula by putting the constraint that the particle is reflected at $r = R_0$ (R_0 being the nuclear radius), instead of infinity. This is an ideal situation for the nuclear shell model, which states that a particle moving in harmonic oscillator mean-field is confined in a spherical cavity of radius R_0. In this work, we have fixed the potential strength with the help of virial theorem. The complete formalism is free from singularities and does not involve any fitting parameter.

A complete trace formula for a particle moving in a three-dimensional harmonic isotropic oscillator mean-field with spin-orbit coupling is given in Sec. 2. Section 3 is devoted to results and discussion. The conclusions are summarized in Sec. 4.

2. Trace formula for isotropic harmonic oscillator mean-field with spin-orbit coupling

For the bound states of a single particle Hamiltonian H, the level density is generally defined as a sum of Dirac delta distributions,

$$g(E) = \sum_i \delta(E - E_i). \qquad (2)$$

This sum runs over all the eigen-energies E_i (including degeneracies). It can split into a smooth and an oscillating part:

$$g(E) = \tilde{g}(E) + \delta g(E). \qquad (3)$$

The oscillating component of the single particle level density $\delta g(E)$, in cylindrical coordinates (ρ, ϕ, z) is given by

$$\delta g(E) = \frac{1}{\pi \hbar^2} \sum_{\beta,m} f_{\beta,m} \sin\left(\frac{S_{\beta,m}}{\hbar} + \alpha_{\beta,m}\right)$$

$$\times \iint d\rho dz \sqrt{|p_\rho \rho J(P_\rho P_z t_{\beta,m}; \rho' z' E)|_{\rho',z' \to \rho,z}}. \qquad (4)$$

The factor $f_{\beta,m}$ equals to 1 for the diametric orbits and 2 for other orbits like triangles, squares, etc. The time-period for the path from the initial point $\vec{r}$ to the final point $\vec{r}''$ for energy E is defined as

$$t_\beta = \frac{\partial S_\beta(\vec{r}, \vec{r}'', E)}{\partial E}. \qquad (5)$$

The quantity J in Eq. (4) is the Jacobian of transformation between two sets of classical quantities $(p_\rho, P_z, t_{\beta,m})$ and (ρ', z', E), which are related by the classical equations of motion. Here, β denotes the type of orbits and m is the number of reoetitions of a given type of orbit.

The periodic orbit sum in Eq. (4) does not converge in most cases. Since the maximum contribution to the gross shell structure comes from the shortest periodic orbits. It has now become customary to carry out a smooth truncation of the contributions of the longer periodic orbits by folding the level density with a Gaussian function [12] of width γ,

$$\delta g_{av} = \sum_{\beta,m} \delta g(E) \exp\left[\left(-\frac{\gamma t_{\beta,m}}{2\hbar}\right)^2\right] \qquad (6)$$

The averaging width γ is chosen to be larger than the mean spacing between the energy levels within a shell, but much smaller than the distance between the gross shells. This averaging ensures that all longer paths are strongly damped and only the shortest periodic orbits contribute to the oscillating part of the level density. Also, the effect of degeneracies is included in Eq. (4) by using the prescription outlined in Ref. [19].

We have approximated the nuclear mean-field by an isotropic harmonic oscillator. The Hamiltonian for a single particle of mass M is expressed in terms of spherical polar coordinates (r, θ, ϕ) and the conjugate momenta (p_r, p_θ, p_ϕ) as

$$H = \frac{1}{2M}\left[P_r^2 + \frac{1}{r^2}p_\theta^2 + \frac{1}{r^2 \sin^2\theta}p_\phi^2\right] + \frac{1}{2}M\omega^2 R^2. \qquad (7)$$

Equation (7) leads to a Hamilton-Jacobi equation, which can be solved by using the separation of variable technique.

Therefore, the classical dynamics of a particle is determined by the following three partial actions:

$$s_\theta = \oint d\theta \sqrt{\varepsilon^2 - \frac{l_z^2}{\sin^2\theta}} = 2\pi(\varepsilon - l_z), \qquad (8)$$

$$s_r = \oint dr \sqrt{2ME - M^2\omega^2 r^2 - \frac{\varepsilon^2}{r^2}}, \qquad (9)$$

$$s_\phi = 2\pi l_z. \qquad (10)$$

Here, ε and l_z are the separation constants and are obtained from the following periodicity conditions.

$$\frac{\omega_r}{\omega_\theta} = \frac{\partial s_\theta/\partial\varepsilon}{\partial s_r/\partial\varepsilon} = \frac{n_r}{n_\theta} \qquad (11)$$

$$\frac{\omega_\phi}{\omega_\theta} = -\frac{1}{2\pi}\left[\frac{\partial s_\theta}{\partial l_z} + \frac{\partial s_r/\partial l_z}{\omega_\theta/\omega_r}\right] = \frac{n_\phi}{n_\theta} \qquad (12)$$

The integration in the r-coordinate of Eq. (9) is obtained analytically under two limiting approximations: (i) the upper limit lies at infinity and (ii) it lies at R_0. Both these cases are discussed in the following subsections.

2.1. Case I: upper bound lies at infinity

The limits of radial integration are determined by the reflection points which, in turn, are obtained by solving the equation

$$p_r^2 = 2ME - M^2\omega^2 R^2 - \frac{\varepsilon^2}{r^2} = 0. \qquad (13)$$

Since the radial coordinate is positive, so we consider the following positive roots of equation (13) for the lower and upper limits of the integration in Eq. (4.9).

$$r_{\min} = \sqrt{\frac{E}{M\omega^2}\left[1 - \sqrt{\sigma_2}\right]}, \qquad (14)$$

$$r_{\max} = \sqrt{\frac{E}{M\omega^2}\left[1 + \sqrt{\sigma_2}\right]}, \qquad (15)$$

with $\sigma_2 = \varepsilon^/(E/\omega)^2$, a dimensionless constant. Thus the action in the radial coordinate becomes

$$s_r = \pi\frac{E}{\omega}(1 - \sqrt{\sigma_2}). \qquad (16)$$

The first periodicity condition Eq. (11) implies $\omega_r = 2\omega_\theta$, *i.e.*, only the pendulating orbits are possible, which confirms the result of Bohr and Mottelson [28]. The second condition fixes $\omega_\theta = \omega_\phi$. These constraints clearly indicate that both separation constants ε and l_z are constants of motion.

Thus the total action in Eq. (4) is obtained as

$$s_\beta = n_r s_r + n_\theta s_\theta + n_\phi s_\phi = n_r\pi\frac{E}{\omega}. \qquad (17)$$

The Maslov index $\alpha_{\beta,m}$ in Eq. (4), plays a very crucial role in the periodic sum as it decides the relative phase of the various terms in the summation. Following Creagh and

Littlejohn [29] and Brack and Bhaduri [12], we obtain the following Maslov indices for the pendulating orbits.

$$\alpha_{\beta,m} = -\frac{3}{2}mn_r\pi. \qquad (18)$$

Finally, the Jacobian in Eq. (4) is calculated numerically using the procedure outlined in Ref. [20]. The calculations of Jacobian involve the generalized radial, and axial coordinates ρ, z respectively and their generalized momenta. These generalized coordinates are defined as :

$$\rho = r\sin\theta, \quad z = r\cos\theta. \qquad (19)$$

The corresponding canonically conjugate momenta p_ρ and p_z are

$$p_\rho = \sqrt{2ME - M^2\omega^2 R^2 - \frac{\varepsilon^2}{R^2}}\,\sin\theta$$
$$+ \frac{1}{r}\cos\theta\sqrt{\varepsilon^2 - \frac{l_z^2}{\sin^2\theta}} \qquad (20)$$

$$p_\rho = \sqrt{2ME - M^2\omega^2 R^2 - \frac{\varepsilon^2}{R^2}}\,\cos\theta$$
$$- \frac{1}{r}\cos\theta\sqrt{\varepsilon^2 - \frac{l_z^2}{\sin^2\theta}} \qquad (21)$$

These quantities are inserted in Eq. (4) to calculate the fluctuating part of the level density.

The smooth part of the density of states is calculated within the Thomas-Fermi approximation and is given by

$$\tilde{g}(E) = \frac{1}{2\pi^2}\left(\frac{2M}{\hbar^2}\right)^{3/2}\int d^3r\,\sqrt{E - V(\vec{r})}\,\Theta(E - V). \qquad (22)$$

The Eq. (22) has already been multiplied by a factor of 2 to include the spin degeneracy. For the harmonic oscillator potential, $V = (1/2)m\omega^2 r^2$, the integral is evaluated analytically, and we obtain $\tilde{g}(E) = E^2/(\hbar\omega)^3$.

The harmonic potential with asymptotic reflection point at infinity generates only the pendulating trajectory (*i.e.* $l = 0$. A significant contribution of $\vec{l}\cdot\vec{s}$ coupling arises due to the availability of trajectories with $l \neq 0$. Such trajectories with $l \neq 0$ are obtained in our formalism by fixing the upper bound at R_0 (as discussed in the following subsection).

2.2. Case II: The upper reflection point at R_0

In this case, the particle motion is bounded between an upper limit provided by the radius of sphere $r = R_0$ and a lower limit fixed at $r_{\min}$ (see Eq. (14)). It is worthwhile to mention here that such a scenario corresponds to a particle enclosed in a spherical cavity with perfectly reflecting walls. The radial action, given by Eq. (9), becomes:

$$s_r = \sqrt{2MER_0}\left[\sqrt{1 - \sigma_1 - \sigma_2} - \sqrt{\sigma_2}\left(\sin^{-1}\frac{1 - 2\sigma_2}{\sqrt{1 - 4\sigma_1\sigma_2}}\right.\right.$$
$$\left.\left. + \frac{\pi}{2}\right) - \frac{1}{2\sqrt{\sigma_1}}\left(\sin^{-1}\frac{1 - 2\sigma_1}{\sqrt{1 - 4\sigma_1\sigma_2}} - \frac{\pi}{2}\right)\right]. \qquad (23)$$

TABLE I. A comparison of eigenvalues, in terms of kR_0, of an isotropic oscillator of Case II, without and with $\vec{l} \cdot \vec{s}$ coupling.

n	l	Qmech. no. $\vec{l} \cdot \vec{s}$	Scl. no. $\vec{l} \cdot \vec{s}$	Scl. $+ \vec{l} \cdot \vec{s}$	Scl. $- \vec{l} \cdot \vec{s}$
1	s	3.142	3.138	3.124	3.151
1	p	4.493	4.524	4.483	4.566
1	d	5.763	5.834	5.762	5.906
2	s	6.283	6.333	6.320	6.345
1	f	6.988	7.104	6.999	7.209
2	p	7.725	7.801	7.762	7.841
1	g	8.183	8.349	8.210	8.489
2	d	9.095	9.201	9.134	9.268
3	s	9.356	9.515	9.403	9.520
1	h	9.425	9.577	9.502	9.753
2	f	10.417	10.557	10.461	10.653
1	i	10.513	10.794	10.582	11.007
3	p	10.904	11.017	10.978	11.056
2	g	11.657	11.881	11.754	12.008

Here, $\sigma_1 = (M\omega^2 R_0^2)/2E$ is a dimensionless constant and refers to potential strength. Another dimensionless constant $\sigma_2 = \varepsilon^2/(2MER_0^2)$ is related to the separation constant ε and is fixed by the periodicity condition Eq. (11) as

$$\frac{1}{2}\left[\sin^{-1}\frac{1 - 2\sigma_2}{\sqrt{1 - 4\sigma_1\sigma_2}} + \frac{\pi}{2}\right] = \pi\frac{n_\theta}{n_r}. \tag{24}$$

The periodicity condition Eq. (12) gives $\omega_\theta = \omega_\phi$, which implies that l_z is again a constant of the motion. This gives us the trajectories with $l \geq 0$. The constant, σ_1 is fixed by using the virial theorem as discussed below.

We know that $2T = \sum_i p_i \dot{q}_i$ (T is the kinetic energy of the system; q_i and p_i are the generalized coordinates and momenta, respectively). Integrating both sides concerning time over a complete period of motion and also using the virial theorem $\bar{T} = \bar{V}$ we get

$$\frac{1}{2\sqrt{\sigma_1}} = \sqrt{1 - \sigma_1 - \sigma_2} - \frac{1}{2\sqrt{\sigma_1}}$$
$$\times \left[\sin^{-1}\frac{1 - 2\sigma_1}{\sqrt{1 - 4\sigma_1\sigma_2}} - \frac{\pi}{2}\right]. \tag{25}$$

Here, the bar on the physical quantities T and V refer to an average over a single period of motion. Thus the total action in (4) is obtained as

$$S_\beta = \sqrt{2MER_0}n_r\left[\sqrt{1 - \sigma_1 - \sigma_2} - \frac{1}{2\sqrt{\sigma_1}}\right.$$
$$\left.\times\left(\sin^{-1}\frac{1 - 2\sigma_1}{\sqrt{1 - 4\sigma_1\sigma_2}} - \frac{\pi}{2}\right)\right] \tag{26}$$

The Maslov index $\alpha_{\beta,m}$, in this case, is given by the following expressions:

For diametric orbits ($l = 0$ trajectories),

$$\alpha_{\beta,m} = -\frac{3}{2}mn_r\pi. \tag{27}$$

For other orbits ($l = 0$ trajectories),

$$\alpha_{\beta,m} = -\frac{3}{2}mn_r\pi - (mn_\theta - 1)\pi + \frac{3\pi}{4} \tag{28}$$

Here, also the Jacobian is calculated by using the procedure as discussed in case I.

Next, the maximum limit for the repetition parameter m in Eq. (4) is obtained by considering that the longest periodic orbit, out of the permissible families β, traverses only once in the cavity. This fixes the repetition numbers of the individual families concerning that of the largest one, i.e.

$$m_{max} = \frac{L_{l\,arg\,est}}{L_\beta(n_r, n_\theta, n_\phi)} \tag{29}$$

The length of the orbit L_β, is related to the action S_β by the relation

$$S_\beta = \sqrt{2MEL_\beta}. \tag{30}$$

Thus, the fluctuating part of the level density is fully established by including all the above mentioned terms in Eq. (4).

Finally, the smooth part is obtained by using the spherical cavity considerations [30]

$$\tilde{g}(E) = \frac{1}{4\pi^2}\left(\frac{2M}{\hbar^2}\right)^{3/2}\sqrt{EV} - \frac{1}{16\pi}\left(\frac{2M}{\hbar^2}\right)S$$
$$+ \frac{1}{12\pi^2}\left(\frac{2M}{\hbar^2}\right)^{1/2}\frac{C}{\sqrt{E}}, \tag{31}$$

where, V, S, and C refer to the volume, surface area, and radius of curvature of the spherical cavity, respectively.

2.3. Inclusion of $\vec{l} \cdot \vec{s}$ coupling term

The Hamiltonian, H, in Eq. (7) is modified by including the $\vec{l} \cdot \vec{s}$ coupling. This coupling term is defined as

$$\vec{l} \cdot \vec{s} = \frac{1}{2}[l_x \sigma_x + l_y \sigma_y + l_z \sigma_z]. \tag{32}$$

This equation is a 2×2 matrix, which is diagonalized to obtain two eigenvalues:

$$\langle \vec{l} \cdot \vec{s} \rangle = \pm \frac{1}{2} \sqrt{l^2 - l_z}\hbar. \tag{33}$$

In spherical polar coordinates, l^2 and l_z are expressed as

$$l^2 = p_\theta^2 + \frac{1}{\sin^2 \theta} p_\phi^2, \tag{34}$$

$$l_z = p_\phi. \tag{35}$$

These generalized momenta are represented in terms of derivative of partial actions concerning their generalized coordinates, we have

$$\langle \vec{l} \cdot \vec{s} \rangle = \pm \frac{1}{2} \sqrt{\left(\frac{ds_\theta}{d\theta}\right)^2 + \frac{1}{\sin^2 \theta}\left(\frac{ds_\phi}{d\theta}\right)^2 - \hbar \frac{ds_\phi}{d\phi}}. \tag{36}$$

Further, using Eqs. (8-10), we get

$$\langle \vec{l} \cdot \vec{s} \rangle = \pm \frac{1}{2} \sqrt{\varepsilon^2 - l_z}\hbar \approx \pm \frac{1}{2}\varepsilon. \tag{37}$$

The contribution of $l_z \hbar / \varepsilon^2$ is extremely small and hence can be neglected. We have fixed the coupling strength κ as follows:

$$\kappa = -\lambda \left(\frac{\hbar}{Mc}\right)^2 \frac{1}{r}\frac{\partial V}{\partial r} = -\lambda \sqrt{\sigma_1} \tag{38}$$

Remarkably, the spin-orbit coupling constant is related to the harmonic oscillator potential constant σ_1, which makes our formalism free from the fitting procedure. Here, λ is a dimensionless constant, and its value is taken equal to 0.2 for a reasonable splitting in the eigenvalue spectrum.

The inclusion of $\vec{l} \cdot \vec{s}$ coupling term modifies the energy in the Hamilton Jacobi equation to $E \pm (\kappa/2)\varepsilon$. This modified energy is used in Eq. (9) to obtain the radial action s_r, which is further used in obtaining the periodicity constraints and hence the fluctuating part of the level density.

The periodicity condition (Eq. (11)) thus calculated by using the formalism for the case I gives $\omega_r = (2\omega_\theta / 1 \mp (\lambda/2))$. This clearly indicates that ε is again a constant of the motion and gives trajectories with $l = 0$. So, case I does not contribute significantly to spin-orbit splitting. On the other hand, this condition, within case II, gives

$$\frac{1}{2}\left[\sin^{-1}\frac{1 \mp \lambda \sqrt{\sigma_1 \sigma_2} - 2\sigma_2}{\sqrt{(1 \mp \lambda \sqrt{\sigma_1 \sigma_2})^2 - 4\sigma_1 \sigma_2}} + \frac{\pi}{2}\right] \mp \frac{1}{4}\lambda$$

$$\times \left[\sin^{-1}\frac{1 \mp \lambda \sqrt{\sigma_1 \sigma_2} - 2\sigma_2}{\sqrt{(1 \mp \lambda \sqrt{\sigma_1 \sigma_2})^2 - 4\sigma_1 \sigma_2}} - \frac{\pi}{2}\right] = \pi\frac{n_\theta}{n_r} \tag{39}$$

The mean-field strength also gets modified by the inclusion of $\vec{l} \cdot \vec{s}$ coupling as follows,

$$\frac{1}{2\sqrt{\sigma_1}} = \sqrt{1 \mp \lambda \sqrt{\sigma_1 \sigma_2} - \sigma_1 - \sigma_2} - \frac{1}{2\sqrt{\sigma_1}}$$

$$\times \left[\sin^{-1}\frac{1 \mp \lambda \sqrt{\sigma_1 \sigma_2} - 2\sigma_2}{\sqrt{(1 \mp \lambda \sqrt{\sigma_1 \sigma_2})^2 - 4\sigma_1 \sigma_2}} - \frac{\pi}{2}\right] \tag{40}$$

These conditions together generate trajectories by varying n_θ and n_r, which correspond to orbits with $l \geq 0$. Therefore, the spin-orbit coupling shows up significant splitting in our eigenvalue spectrum.

3. Results and discussion

Firstly, we discuss the semiclassical eigenvalue spectrum of isotropic harmonic oscillator without $\vec{l} \cdot \vec{s}$ coupling. Further, the numerical results of case I are presented first. In this case, we have varied n_θ from 1 to 500. The periodicity conditions (Eqs. (11) and (12)) fix $n_r(= 2n_\theta)$ and $n_\phi(= n_\theta)$, respectively. Since only one type of orbits, known as diametric orbits are involved, the repetition parameter m is kept equal to 1. The averaging width γ is chosen as 0.002 for proper convergence of the sum in Eq. (4). Here, the energy is measured in units of $\hbar\omega$. The results of $g(E)$ vs. E are shown in Fig. 1. It is interesting enough to note that the peak positions coincide exactly with those of the quantum levels $E_N = (N + (3/2))\hbar\omega$
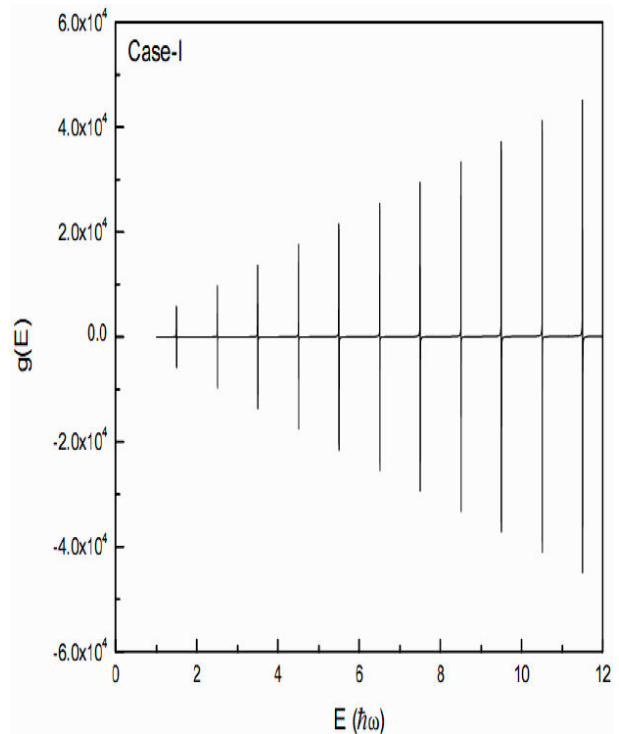

FIGURE 1. Total level density $g(E)$ vs. E in units of $\hbar\omega$ for Case I of isotropic oscillator.
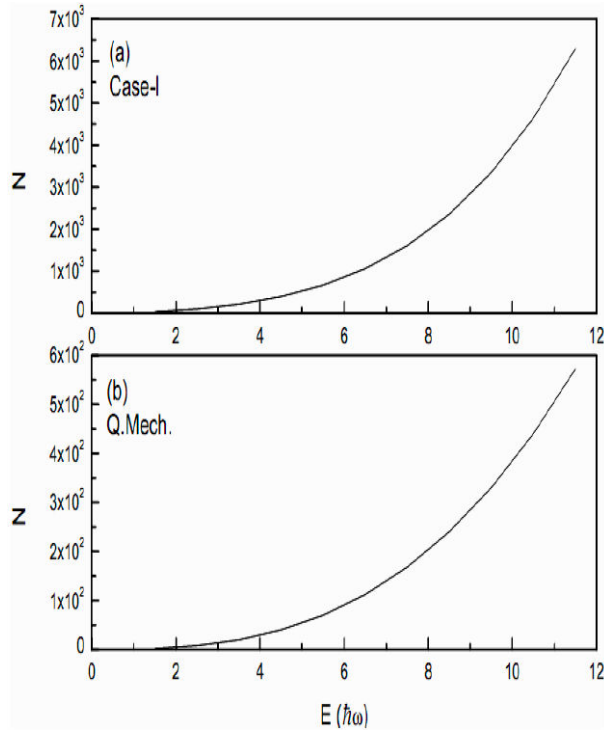
FIGURE 2. (a) Particle number N vs. E in units of $\hbar\omega$ for Case I of isotropic oscillator. (b) Plot of Quantum results.

FIGURE 3. Total level density $g(E)$ vs. kR_0 for Case II of isotropic oscillator with $\kappa = 0$. The quantum results are also given for comparison.

(with $N = 0, 1, 2, 3$ etc.) and peak heights resemble nearly with the quantum mechanical degeneracies $(1/2)(N + 1)(N + 2)$. Here, we would like to mention that the difference between the semiclassical eigenvalues and quantum mechanical ones is 2×10^{-3}. An analytically exact result was already obtained in Ref. [15] by modifying the Gutzwiller's trace formula for stable orbits. It is worthwhile to mention here that the frequency ratios in our approach are fixed by the periodicity conditions. Also, the trajectories fixed by the periodicity conditions in our approach fully support the observation made by Bohr and Mottelson [28] that only the pendulating orbits are possible in an isotropic harmonic oscillator potential.

The number of particles are obtained by using the relation:

$$N = \int_0^{E_F} g(E)dE. \tag{41}$$

Here, E_F refers to energy corresponding to the peak position in Fig. 1 and $g(E)$ is the total level density. The calculated results of N vs. E are shown in Fig. 2. The quantum mechanical results are also shown in this figure. A comparison of semiclassical results with those of quantum mechanical ones shows a remarkable similarity in the variation of N vs. E. However, the semiclassical values are an order of magnitude higher than the quantum mechanical values. This order of magnitude can be reduced by incorporating the Pauli-principle in the trace formula [31]; it is not included here. The diametric trajectories c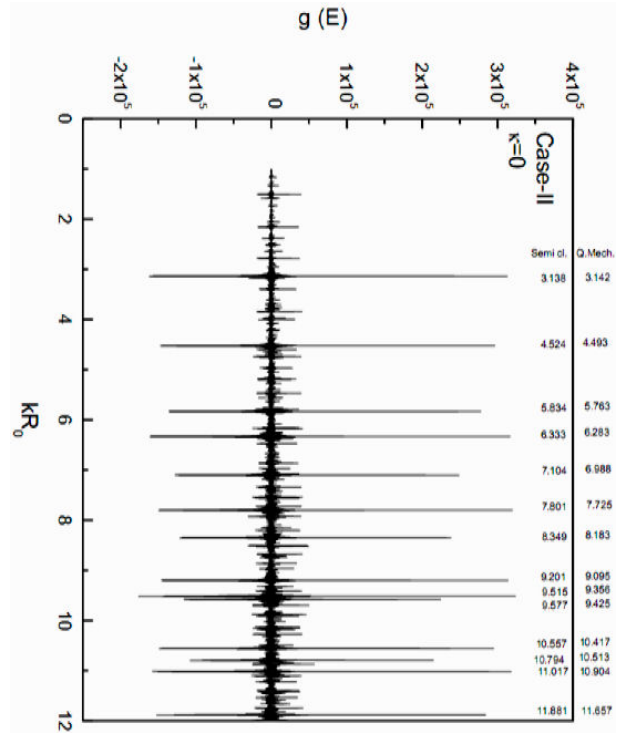orrespond to $l = 0$ contribution and hence do not reproduce splitting by including the $\vec{l} \cdot \vec{s}$ coupling (as discussed above in Sec. 2.3).

To obtain the splitting due to $\vec{l} \cdot \vec{s}$ coupling, we have switched over to case II. In this case, we have varied both n_θ from 1 to 500 and n_r from $2n_\theta$ to 500, whereas n_ϕ is fixed equal to n_θ by using the periodicity condition Eq. (12). These varied integers are used in Eq. (24) to obtain trajectories with $l \geq 0$. Further, we have solved simultaneously the transcendental Eqs. (24) and (25) to ascertain the shapes of trajectories possible in the harmonic oscillator mean-field. Here, γ is again fixed equal to 0.002, and the upper limit of the repeated orbits, m_{max} is obtained by Eq. (29). We have already pointed out that this scenario resembles a spherical cavity problem. Therefore, we have calculated the energies in units of $\hbar^2/2MR_0^2$. The results of $g(E)$ vs kR_0 (where $k = \sqrt{2ME}/\hbar$) are shown in Fig. 3. It is obvious that the peak positions show a similar eigenvalue spectrum as observed in a spherical cavity [30], and are fairly close to the zeroes of Bessel functions (which are the quantum mechanical results of a single particle confined in spherical potential well). Here, we would like to point out that for an exact comparison with the quantum mechanical results, one has to solve the quantum mechanical eigenvalue equation for such a truncated mean field at R_0.

The particle numbers are calculated by using Eq. (41) and are shown in Fig. 4 as a function of kR_0. Here, F_F in terms of kR_0 is varied continuously from 1 to 12. Again the calculated N values are quite high as compared to quantum results,
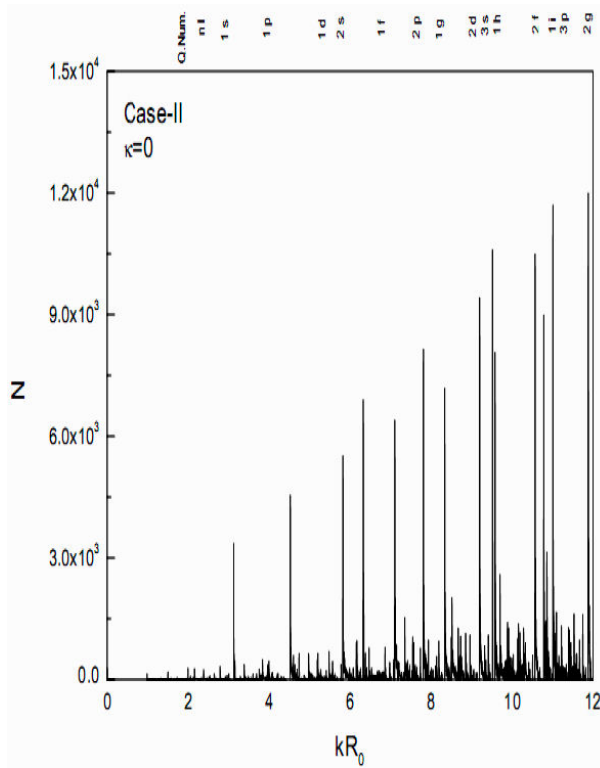
FIGURE 4. Particle number N vs. kR_0 for Case II of isotropic oscillator with $\kappa = 0$.

FIGURE 5. Total level density $g(E)$ vs. kR_0 for combination of Case II and positive sign with k in $\vec{l} \cdot \vec{s}$ coupling.

which can be reduced by including Pauli-principle in the trace formula. If we compare this plot with the quantum numbers which are also identified at the top of this plot, the following interesting features emerge:

(i) The significant gaps in the kR_0 values are seen at the usual magic numbers of the spherical well, *i.e.*, 2, 8, 20, 34, 58, 92 and 138.

(ii) The relative difference in peak heights referring to the quantum shells $1s$, $1p$ $1d$, $1f$, $1g$, $1h$, and $1i$ is constant and is equal to 1 unit each. The relative increase of one unit in the peak height concerning its predecessor refers to the increase in angular momentum by one unit.

(iii) A sudden rise in the number peak among the nearest neighbors indicate the existence of a shell with a different quantum number 'n'.

(iv) The repetition of a particular shell occurs in the spectrum at a particular value of kR_0, if the relative ratio of the peak heights coincides with their respective ratio of kR_0. For example, the ratio of peak heights of 2 and 1 is 2, which is the same as their ratios of kR_0 values. Hence from this analysis, the quantum number 'n' can be identified.

Another advantage of this study is to show the splitting of the eigenvalue spectrum by including the $\vec{l} \cdot \vec{s}$ coupling in the
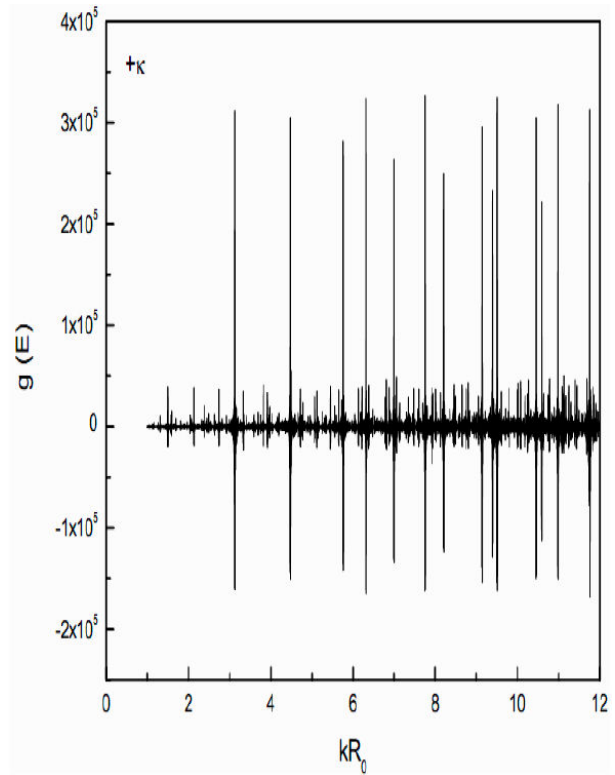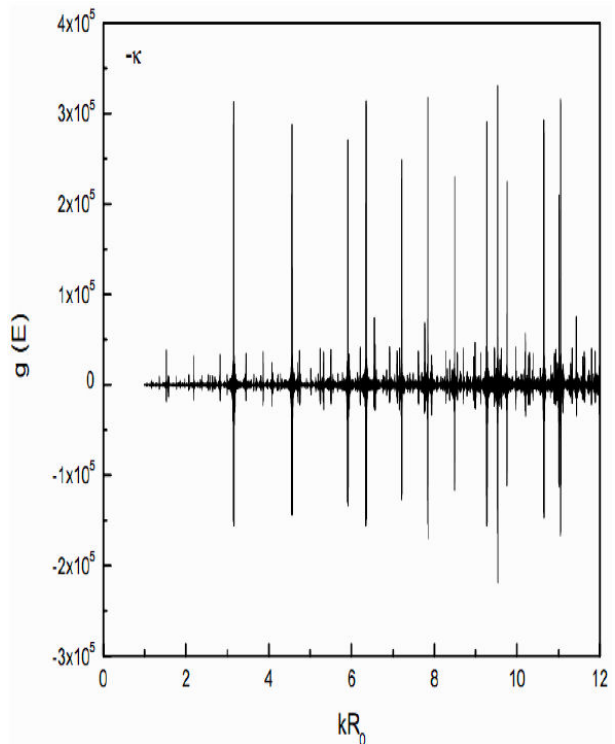

FIGURE 6. Total level density $g(E)$ vs. kR_0 for Case II and negative sign with κ in $\vec{l} \cdot \vec{s}$ coupling.
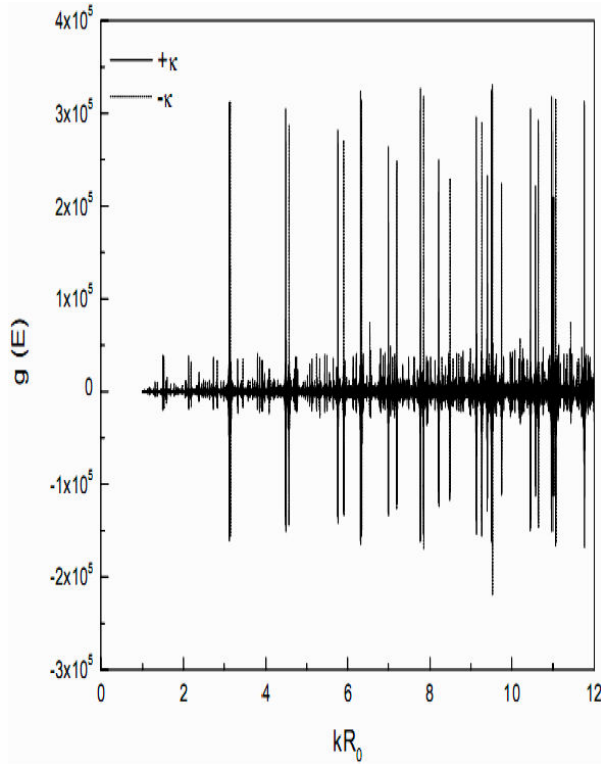
FIGURE 7. Total level density $g(E)$ vs. kR_0 for Case II including both positive and negative signs with κ in $\vec{l} \cdot \vec{s}$ coupling.

FIGURE 8. Particle number N vs. kR_0 for Case II including both positive and negative signs with κ in $\vec{l} \cdot \vec{s}$ coupling.

nuclear mean-field. The inclusion of $\vec{l} \cdot \vec{s}$ coupling involves positive as well as negative signs with κ in the quantities used for calculation of the fluctuating part of the level density. Figures 5 and 6 show the results of total level density, $g(E)$, as a function of positive and negative signs with kR_0 in Sec. 2.3), respectively. These results are also tabulated in Table I together with the quantum mechanical results of the spherical cavity without $\vec{l} \cdot \vec{s}$ coupling. The semiclassical results without $\vec{l} \cdot \vec{s}$ coupling are also given in this table. On comparing the results of positive and negative contributions, it is observed that the eigenvalues corresponding to negative sign are higher as compared to those of positive sign. Further, a comparison of these eigenvalues with the results of the harmonic oscillator (Case II) having zero $\vec{l} \cdot \vec{s}$ coupling shows that each level is split into two. The splitting width of each level is consistent with the quantum mechanical results as discussed below.

In nuclear system with $\vec{l} \cdot \vec{s}$ coupling, we get two eigenvalues for each angular momentum l, which are equal to $-\kappa \times l$ for $j = l + (1/2)$ and $\kappa \times (l + 1)$ for $j = l - (1/2)$. A similar splitting is observed in our semiclassical approach. The quantum spectrum does not split the eigenvalue corresponding to $l = 0$ level, whereas in semiclassical calculations each level is splitted into two. It is quite interesting to note in Table I that, corresponding to each quantum mechanical s-state, the semiclassical splitting is extremely small ~ 0.027 as compared to other states. Also, the splitting width ΔE is nearly proportional to $(2l + 1)$ the s-state splitting for each l (where l refers to the quantum number in Table I). It is a remarkable
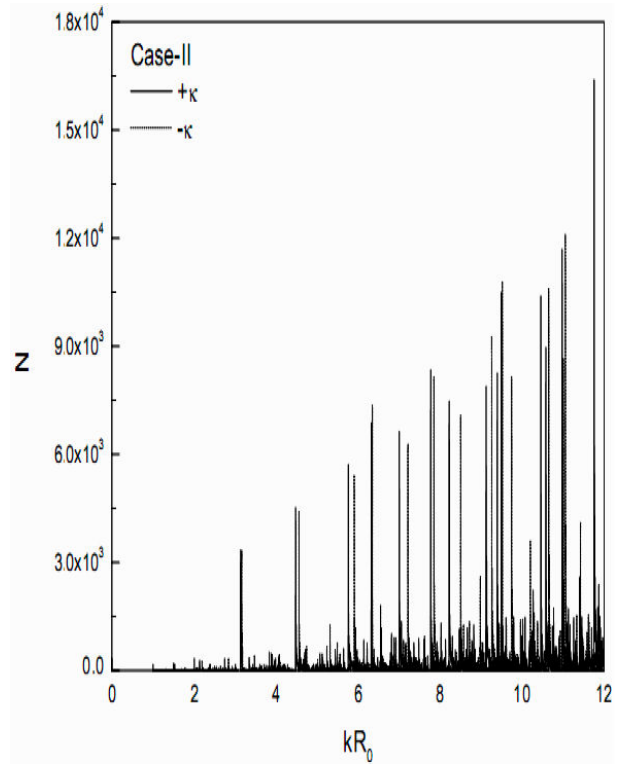
observation and fully supports the nuclear shell model spectrum. Further, it is noticed that the simultaneous solution of Eqs. (39) and (40) with the minus sign gives the diametric orbits, whereas no such trajectories are seen with the positive sign. These diametric orbits refer to $l = 0$ as pointed out by Bohr and Mottelson [28]. Therefore, its absence in one choice of sign (+), leads to a small splitting in the s-state.

Finally, the total level density $g(E)$ vs kR_0, including both positive and negative signs with κ, is shown in Fig. 7, respectively, by solid and dotted curves. The resultant eigenvalue spectrum clearly shows the splitting.

The plot of the number of particles, $vs\ kR_0$ with both positive and negative signs of κ are shown by solid and dotted curves, respectively, in Fig. 8. It is evident from this plot that the dotted curve refers to the quantum mechanical case of $j = l - (1/2)$, whereas the solid curves refer to $j = l + (1/2)$. The number of particles shown by the dotted curve is less than those of a solid curve in a particular shell, which again supports the quantum mechanical observation. In order to get a reasonable separation in kR_0 at the magic numbers 28, 50, etc., we have to adjust the splitting parameter λ, which we have chosen equal to 0.2. Thus a complete semiclassical picture of the nuclear shell model is obtained, which will help predic the next magic numbers.

4. Conclusion

A trace formula for the level density of an isotropic harmonic oscillator with $\vec{l} \cdot \vec{s}$ coupling is presented. Our formalism re-

produces the eigenvalue spectrum of pure quantum oscillator exactly. The contribution of angular momentum is generated by terminating the upper limit at the nuclear radius R_0, which fully reproduces the resultant nuclear spectrum with $\vec{l} \cdot \vec{s}$ coupling. We have established the role of significant quantum numbers 'n' and 'l' in this semiclassical method. The overall eigenvalue spectrum compares reasonably well with that of the nuclear shell model (with magic numbers) without any fitting parameter.

Acknowledgments

1. Amita, A.K. Jain and B. Singh, *Atomic Data and Nuclear Data Tables* **74** (2000) 283.

2. S. Frauendorf, *Review of Modern Physics* **73** (2000) 463.

3. A.K. Jain, R.K. Sheline, P.C. Sood and K. Jain, *Review of Modern Physics* **62** (1990) 393.

4. S. Lakshmi, H.C. Jain, P.K. Joshi, A.K. Jain and S.S. Malik, *Physical Review C* **69** (2004) 014319.

5. S. Hofmann and G.Munzenberg, *Review of Modern Physics* **72** (2000) 733.

6. C. Baktash, B. Hass and W. Nazarewicz, *Annual Reviews Nuclear and Particle Science* **45** (1995) 485.

7. V.M. Strutinsky, *Nuclear Physics A* **95** (1967) 420; ibid **122** (1968) 1.

8. M. Brack, J. Damgard, A.S. Jensen, H.C. Pauli, V.M. Strutinsky and C.Y. Wong, *Review of Modern Physics* **44** (1972) 320.

9. S. Bjornholm and J.E. Lynn, *Review of Modern Physics* **52** (1980) 725.

10. M.C. Gutzwiller, *J. Math. Phys.* **8** (1967) 1979; ibid **10** (1969) 1004; ibid **11** (1970) 1791; ibid **12** (1971) 343.

11. R. Balian and C. Bloch, *Ann. Phys. (NY)* **60** (1970) 401; ibid **69** (1972) 76.

12. See for details. M. Brack and R.K. Bhaduri, *Semiclassical Physics* (Addison Wesley, Reading, 1997).

13. S.R. Jain, *Journal of Physics G: Nuclear and Particle Physics* **30** (2004) 157.

14. M.C. Gutzwiller, *Chaos in Classical and Quantum Mechanics*. Springer-Verlag, New York (1990).

15. M. Brack and S.R. Jain, *Physical Review A* **51** (1995) 3462.

16. S.C. Creagh and R.G. Littlejohn, P*hysical Review A* **44** (1991) 836; *J. Phys. A* **25** (1992) 1643.

17. S.C. Creagh, *Ann. Phys. (NY)* **248** (1996) 60.

18. M. Brack, S.C. Creagh and J. Law, *Physical Review A* **57** (1998) 788.

19. V.M. Strutinsky, *Nucleonica* **20** (1975) 679; V.M. Strutinsky and A.G. Magner, *Soviet Journal of Particles and Nuclei* **7** (1977) 138; V.M. Strutinsky and A.G. Magner, S.R. Ofengenden and T. Dossing, *Zeitschrift fur Physik A* **283** (1977) 269.

20. S.S. Malik, A.K. Jain, and S.R. Jain, *International Journal of Modern Physics E* **11** (2002) 303.

21. S.A. Moskowski, *Physical Review* **99** (1955) 803.

22. A.G. Magner, S.N. Fedotkin, F.A. Ivanyuk, P. Meier, M. Brack, S.M. Reimann and H. Koiznmi, *Annalen der Physik (Leipzig)* **509** (1997) 555.

23. M. Brack, S.M. Reimann, and M. Sieber, *Physical Review Letters* **79** (1997) 1817.

24. Ch. Amann and M. Brack, *Journal of Physics A* **35** (2002) 6009.

25. R.G. Littlejohn and W.G. Flynn, *Physical Review A* **44** (1991) 5239.

26. R.G. Littlejohn and W.G. Flynn, *Physical Review A* **45** (1992) 7697.

27. H. Frisk and T. Guhr, *Annals of Physics* **221** (1993) 229.

28. A. Bohr and B.R. Mottelson, *Nuclear Structure* (Benjamin, 1975) Vol II.

29. S.C. Creagh and R.G. Littlejohn, *Physical Review A* **42** (1990) 1907.

30. S.S. Malik, M. Dudeja, A.K. Jain, *Pramana Journal of Physics* **53** (1999) 243, and references therein.

31. H.A. Weidenmuller, *Physical Review A* **48** 1819.